

## Theory of helical structures of tilted chiral lipid bilayers

Ou-Yang Zhong-can

*Chinese Center of Advanced Science and Technology (World Laboratory), P.O. Box 8730, Beijing, China  
and Institute of Theoretical Physics, Academia Sinica, P.O. Box 2735, Beijing 100080, China*

Liu Jixing

*Institute of Theoretical Physics, Academia Sinica, P.O. Box 2735, Beijing 100080, China*

(Received 26 November 1990)

Analogous to the theory of cholesteric liquid crystal, a theory for tilted chiral lipid bilayers (TCLB) [briefly reported in *Phys. Rev. Lett.* **65**, 1679 (1990)] is developed. The tilt equation and the surface-shape-equilibrium equation have been derived. Application of the theory shows that on a cylindrical surface, the field of tilt directions of TCLB molecules forms a right-handed helix with a  $45^\circ$  gradient angle for  $k_2 > 0$  or a left-handed helix with  $-45^\circ$  gradient angle for  $k_2 < 0$ , where  $k_2$  is the chiral curvature modulus of the cholesteric liquid crystal. In addition, there exists another type of helical structure that looks like twisted strips or helicoids. It is also shown that on a spherical surface, the tilt field has at least two singular points. Based on these results, the succession of transitions from a vesicular dispersion to a phase involving helical structures and then to tubes observed in several laboratories can be reasonably explained. The general formula that explains the aggregation of narrow and prolate ribbon structures is derived. By including more terms of elasticity free energy into the theory, the size of the helical structure is obtained and is shown to agree with experimental observations.

### I. INTRODUCTION

The lipid bilayer is an attractive subject as it may serve as a structural model for biological membranes and as scaffolding for synthetic functional systems. Theoretical investigations of lipid bilayers, in the early stages, were devoted to the explanations of the shapes of vesicles (closed membranes). To explain the well-known biconcave-disk shape of red blood cells under normal physiological conditions, Helfrich<sup>1,2</sup> has developed the theory of curvature elasticity of lipid bilayers. In this theory, the elastic energy of curvature per unit area of a bilayer deformed with principal curvatures  $c_1$  and  $c_2$  is written as

$$g_c = \frac{1}{2}k(c_1 + c_2 - c_0)^2 + \bar{k}c_1c_2, \quad (1)$$

where  $k$  is the bending rigidity,  $\bar{k}$  is the elastic modulus of the Gaussian curvature, and  $c_0$  is the spontaneous curvature describing the asymmetry of the membrane or its environment. The approach of this model is based on an analogy with the elastic theory of uniaxial liquid crystals. In fact if one takes the normal of the bilayers as the direction of liquid crystals, the expression (1) can be obtained from the expression of Frank free energy for liquid crystals<sup>3</sup> and  $k, \bar{k}, c_0$  is expressed by Frank elastic constants as

$$k = k_{11}t, \quad \bar{k} = -(k_{22} + k_{24})t, \quad c_0 = k_1/k_{11}t, \quad (2)$$

where  $k_{ij}$  are different Frank elasticity constants and  $t$  is the thickness of the membrane.

Obviously, the above-mentioned theory can only be used in the case in which the more or less flexible hydro-

carbon chains have to be directed in the normal direction of the bilayer, i.e., the case of the  $L_\alpha$  phase of membranes [see Fig. 1(b)]. The cases of tilt of the lipid molecules ( $L_\beta$  phase) and tilt of the chiral molecules ( $L_{\beta^*}$  phase) are beyond the scope of the theory. For treating the latter two cases, a new theory of curvature elasticity is needed.

This work is devoted, in particular, to the theory of  $L_{\beta^*}$  bilayers. The goal of this work is (1) to develop in detail a theory (it has been briefly reported in a recent Letter<sup>4</sup> by us) that can be applied to the case of the  $L_{\beta^*}$  phase of membranes and (2) to apply this theory to shed some light on the recent experimental discovery of the helical structures of various amphiphiles.<sup>5-11</sup>

All the experimental observations<sup>5-11</sup> demonstrated that the chemical structure of component amphiphiles, in particular, their chirality, plays a crucial role in the formation of the helical structures. So far there are two types of helical structures that have been reported. The first type of helical structure looks like a ribbon wound around a cylinder with a spiraling gap. The gap sometimes appears to close up so that the ribbon transforms to a prolate tube. Some tubes were multilamellar and look like soda straws (Fig. 3 in Ref. 9). A remarkable property of this type of helical structures is that the gradient angle  $\varphi$  of the helix always appears to be nearly  $45^\circ$ . Another type of helical structure observed in experiments is the twisted strip or right helicoid which seems to be a crossover from vesicular dispersion to the first type of helical structures [Figs. 1(A)–1(D) of Ref. 5]. Technically, these structures can be used in making electro-optical elements, microelectronic elements, reagent delivery vehicles, and microsurgical materials.<sup>12</sup> A recent significant advance is the successful coating of the tubes with nickel and/or

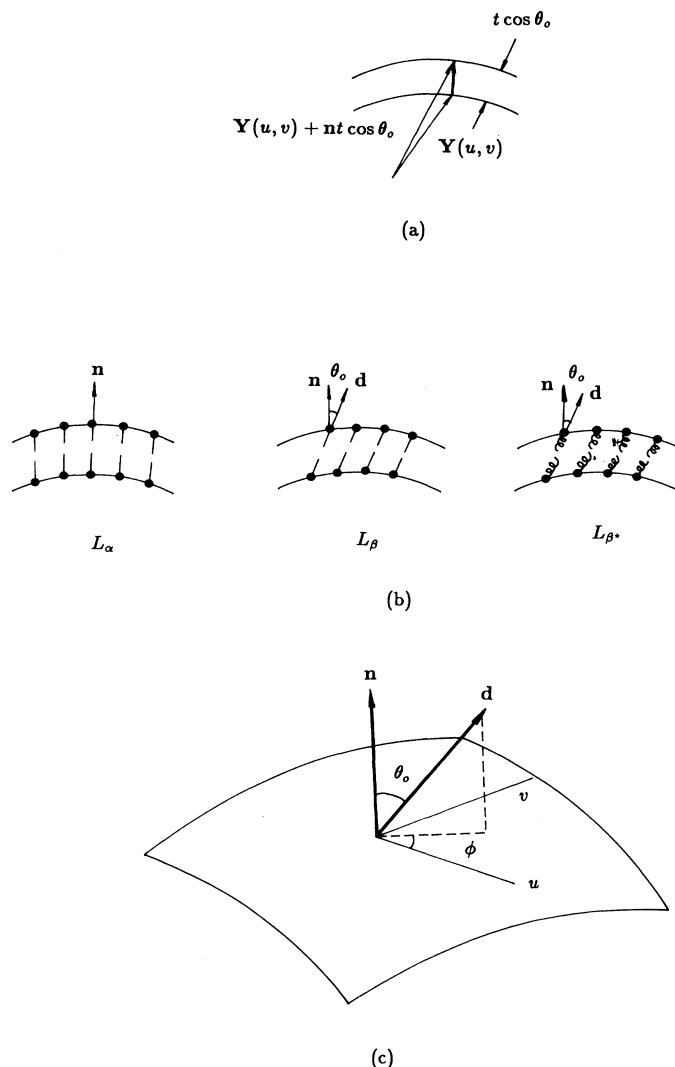


FIG. 1. Configuration of lipid bilayer: (a) geometry of bilayer, (b) molecule directions for the bilayer in different phases, (c) geometry configuration on the curved surface.

copper to make them highly conductive.<sup>13</sup>

On the theoretical side, a major challenge is to understand the mechanism of the winding of the lipid bilayers. The first theoretical treatment of wound-ribbon helices is developed by Helfrich<sup>14</sup> by assuming a competition of a spontaneous torsion of the edges with the bending of membranes. Later the tube formation was also explained by de Gennes in terms of a buckling of flat solid ribbons due to the ferroelectric polarization charges on their edges.<sup>15</sup> Very recently, an improved theory was proposed by Helfrich and Prost<sup>16</sup> in which they employed a new linear term linked to molecular chirality in the bending energy of membranes with  $C_2$  or  $D_2$  symmetry. However, the second type of the observed helical structures, the twisted strips, has not been theoretically handled yet. In addition, the transition from vesicular dispersion to the formation of helical structures observed in experiments

has not been discussed theoretically. And, the size of the helical structures has not been determined by the previous theories yet.

In this paper, different from the above-mentioned approaches, we restrain ourselves in the approach analogous with the Frank theory of uniaxial liquid crystals; in particular, the cholesteric one. By taking into account the effects of chirality of the molecules and the tilt of the director of the liquid crystal, we derive the expression of curvature energy for the tilted chiral lipid bilayers (TCLB). The Euler-Lagrange equations, i.e., the surface-shape-equilibrium equation and the polar-angle equations of the tilt direction, given by variational calculus of the curvature energy, are used to explain the experimental findings mentioned above. The results show that on a cylindrical surface the field of tilt directions of TCLB molecules forms a right-handed helix with a  $45^\circ$  gradient angle

for  $k_2 > 0$  or a left-handed helix with a  $-45^\circ$  gradient angle for  $k_2 < 0$ , where  $k_2$  is the chiral curvature modulus of a cholesteric liquid crystal. Also we found that the right helicoid is a solution of the equations with little higher free energy than that of the cylindrical surface and on a spherical surface, which is also a solution of the surface-equilibrium equation with the highest free energy, the tilt field has at least two singular points. This sequence of free energy for different shapes of membranes may explain the succession of the transition from a vesicular dispersion to a phase involving helical structures and then to a tube observed in experiments. In addition to these results, a general formula in the form of differential geometry for free energy of the TCLB is derived. In this formula the surface integral terms, in the wound-ribbon case, are identical to what is given by Helfrich and Prost,<sup>16</sup> while the other term in the form of a curve integral is a term derived for the first time. Also, using the solutions obtained for the equations derived from the chiral term of free energy to the expression of free energy, including other terms for nematics, the size of the helical structures in agreement with experimental observations is determined theoretically.

The paper is organized as follows. In Sec. II the expression of free energy of the TCLB is derived. In Sec. III the polar-angle equations of tilt directions and the surface-equilibrium equation are given. In Sec. IV the applications of theory to helical structures and sphere are presented. In Sec. V, by adding more terms in the free-energy expression, the tube radius and helical pitch of the helical structures are obtained. In the last section, Sec. VI, a brief summary and some discussions are given.

## II. FREE-ENERGY EXPRESSION FOR TCLB

Theoretically, the membranes of the lipid bilayer may be described as a two-dimensional surface  $\mathbf{Y}(u, v)$  with uniform thickness  $t \cos\theta_0$  [Fig. 1(a)], where  $u, v$  are two real parameters or material coordinates for the membrane. For understanding the distinguished nature in the different phases of the membrane [Fig. 1(b)] at the level of a macroscopic or Frank theory, we note that it is necessary to introduce a number of directions to completely describe the orientation of the molecules. For the simplest case of the  $L_\alpha$  phase, the orientational direction is consistent with the normal of the layer  $\mathbf{n}$ , which is fully determined by the surface  $\mathbf{Y}$  as

$$\mathbf{n} = (\mathbf{Y}_1 \times \mathbf{Y}_2) / \sqrt{g} \quad , \quad (3)$$

where  $\mathbf{Y}_1 = \partial_u \mathbf{Y}$ ,  $\mathbf{Y}_2 = \partial_v \mathbf{Y}$  and  $g = \det(g_{ij})$  with  $g_{ij} = \mathbf{Y}_i \cdot \mathbf{Y}_j$  ( $i, j = 1, 2$ ). It is obvious that in the theory of the  $L_\alpha$  phase, as shown in Eq. (1), there is no need for additional parameters. However, for both the  $L_\beta$  phase [tilted lipid bilayer (TLB)] and the  $L_{\beta^*}$  phase one needs to know the details of the orientational direction  $\mathbf{d}(u, v)$  provided by the tilted angle  $\theta$  and azimuthal angle  $\phi$  as illustrated in Figs. 1(b) and 1(c). The uniform  $L_\beta$  and  $L_{\beta^*}$  phases of the bilayers are generally characterized by constant tilt angle  $\theta = \theta_0$  of the molecule chains with respect to the normal  $\mathbf{n}$  and, in practice, the necessary new parameter is only the scalar function  $\phi(u, v)$ . However, it is not convenient to use  $\phi(u, v)$  straightforward on a curved

surface because it is depending on the curve-coordinate frame of reference. The decisive step taken in the present theory is to use a coordinate-free description of orientation  $\mathbf{d}$  by

$$\mathbf{d} = d_1 \mathbf{Y}_1 + d_2 \mathbf{Y}_2 + \cos\theta_0 \mathbf{n} \quad , \quad (4)$$

where  $d_1$  and  $d_2$  are two scalar functions of  $u, v$ . As in the Frank theory of liquid crystals,  $\mathbf{d}$  is just like the director in liquid crystal and from  $\mathbf{d} \cdot \mathbf{d} = 1$  we have the following relation:

$$g_{ij} d_i d_j - \sin^2\theta_0 = 0 \quad (i, j = 1, 2) \quad . \quad (5)$$

Here and henceforth the repeated indices imply summation over them.

To calculate the free energy of the TCLB with the Frank theory of curvature elasticity, we image the tilted bilayer as a curved liquid-crystal layer sandwiched in between two surfaces  $\mathbf{Y}(u, v)$  and  $\mathbf{Y}(u, v) + t \cos\theta_0 \mathbf{n}(u, v)$ . Given this, it is a relatively straightforward matter to insert Eqs. (4) and (5) into the general expression of the curvature-elastic energy for both nematic and cholesteric liquid crystals. In this way a full formulation of the free energy for both the TLB and the TCLB has been obtained.<sup>17</sup> It is a lengthy and heavy formula related to all the Frank elastic constants; therefore, it is rather difficult to use this formula to analyze the practical structures of the TLB and the TCLB. Since our purpose in this work is to treat the practical problem rather than to give some hard tractable heavy formulas, we turn to analyze the physical aspects of the problem first and then decide which terms of the heavy formula might play an essential role for the problem.

As we pointed out at the beginning, all the experimental observations demonstrated that the chirality of molecules plays a crucial role in the formation of helical structures of the TCLB. Therefore, we should consider the chiral effect as the main ingredient in this theory. In the Frank theory, the chirality of cholesterics is characterized by the following energy-density term:

$$g_{\text{ch}} = -k_2 \mathbf{d} \cdot (\nabla \times \mathbf{d}) \quad , \quad (6)$$

where the minus sign serves to be identical with the original Frank expression. To reveal the role of chirality in the TCLB, for simplicity, we use expression (6) as the energy density of the TCLB instead of the full one. In other words, we discuss the case of the TCLB with a strong chirality effect.

Now we need to transform Eq. (6) to the form closely associated with surface  $\mathbf{Y}(u, v)$ . The first step of the procedure is to represent the three-dimensional gradient operator  $\nabla$  by

$$\nabla = \nabla' + \mathbf{n} \partial_n \quad , \quad (7)$$

where  $\nabla'$  is the two-dimensional gradient operator on the surface  $\mathbf{Y}$  defined by<sup>18</sup>

$$\nabla' = g^{ij} \mathbf{Y}_i \partial_j \quad [g^{ij} \equiv (g_{ij})^{-1}] \quad , \quad (8)$$

and  $\mathbf{n} \partial_n$  is the gradient operator along the direction  $\mathbf{n}$ . The curl of  $\mathbf{d}$  then can be written as

$$\nabla \times \mathbf{d} = \nabla' \times \mathbf{d} + \mathbf{n} \times \partial_n \mathbf{d} \quad . \quad (9)$$

Using Eq. (4), the second term on the right-hand side of Eq. (9) can be expressed as

$$\mathbf{n} \times \partial_n \mathbf{d} = \mathbf{n} \times (d_i \partial_n \mathbf{Y}_i + \cos \theta_0 \partial_n \mathbf{n}) . \quad (10)$$

Because  $\mathbf{n} \cdot \mathbf{n} = 1$ , it follows that

$$\partial_n \mathbf{n} = 0 , \quad (11)$$

but the normal gradient of  $\mathbf{Y}$  does not vanish. With some geometric manipulation one obtains<sup>19</sup>

$$\partial_n \mathbf{Y}_i = -L_{ij} g^{jk} \mathbf{Y}_k , \quad (12)$$

where  $L_{ij}$  is associated with the second fundamental form of the surface  $\mathbf{Y}$  [see below, Eq. (16)]. Equations (11), (12), and (3) then transform Eq. (10) into following form:

$$\mathbf{n} \times \partial_n \mathbf{d} = \epsilon_{3ij} L_{jk} d_k \mathbf{Y}_i / \sqrt{g} . \quad (13)$$

The symbol  $\epsilon_{ijk}$  is defined as

$$\epsilon_{ijk} = \begin{cases} +1, & (ijk) \text{ is an even permutation of } (123) \\ -1, & (ijk) \text{ is an odd permutation of } (123) \\ 0, & \text{otherwise} . \end{cases} \quad (14)$$

The calculation of the two-dimensional curl of  $\mathbf{d}$  needs lengthy derivation; here we simply give the result<sup>20</sup>

$$\nabla' \times \mathbf{d} = \epsilon_{3ji} [(g_{ik} d_{k,j} + g_{il} \Gamma_{kj}^l d_k) \mathbf{n} - L_{jk} d_{k,Y_i}] / \sqrt{g} , \quad (15)$$

where  $d_{k,j} \equiv \partial_j d_k$  and the Christoffel symbols  $\Gamma_{ij}^k$  as well as  $L_{ij}$  are defined by

$$\mathbf{Y}_{ij} = \partial_i \partial_j \mathbf{Y} = \Gamma_{ij}^k \mathbf{Y}_k + L_{ij} \mathbf{n} . \quad (16)$$

From Eqs. (9), (13), and (15) one can get the three-dimensional curl of orientation  $\mathbf{d}$  as

$$\nabla \times \mathbf{d} = \epsilon_{3ji} [g_{ik} (d_{k,j} + \Gamma_{ji}^l d_l) \mathbf{n} - 2L_{jk} d_k \mathbf{Y}_i] / \sqrt{g} . \quad (17)$$

As a simple check, we may consider the case of  $\mathbf{d} \rightarrow \mathbf{n}$ , i.e.,  $\theta_0, d_1, \text{ and } d_2 \rightarrow 0$ . Obviously, in this case Eq. (17) leads to

$$\nabla \times \mathbf{n} = 0 , \quad (18)$$

which is well known in smectics.

By using Eqs. (4), (6), and (17) one can obtain the bulk energy density

$$g_{\text{ch}} = -k_2 \epsilon_{3ji} [\cos \theta_0 g_{ik} (d_{k,j} + \Gamma_{jl}^i d_l) - 2L_{jk} g_{il} d_k d_l] / \sqrt{g} . \quad (19)$$

In order to find the final expressions for the curvature free energy per unit area of the TCBL, we use the following approximation:

$$F = \int g_{\text{ch}} dV = t \cos \theta_0 \int g_{\text{ch}} dA , \quad (20)$$

where  $dV$  is the volume element of the bulk TCLB,  $dA$  is the area element of surface  $\mathbf{Y}$ . Since the thickness  $t \cos \theta_0$  of the TCLB is about twice of the length of the amphiphilic molecule (i.e.,  $t/2$ ) and it is negligibly small in comparison with the linear size of the membrane, the ap-

proximation we used to give Eq. (20) is a reasonable one. Given this, we may conceive the total curvature free energy of the TCLB by

$$F = \int g_{\text{TCLB}} dA \quad (21)$$

with the surface density of free energy

$$g_{\text{TCLB}} = -k_2 t \cos \theta_0 \epsilon_{3ji} [\cos \theta_0 g_{ik} (d_{k,j} + \Gamma_{jl}^i d_l) - 2L_{jk} g_{il} d_k d_l] / \sqrt{g} + \lambda(u, v) (g_{ij} d_i d_j - \sin^2 \theta_0) . \quad (22)$$

The last term in Eq. (22) comes from the constraint Eq. (5). In physics, the Lagrange function  $\lambda(u, v)$  may be explained as a tension stress which, varying with the position on the surface, is indeed induced by the coupling of molecule tilt and the surface curvature.

### III. TILT AND SURFACE-EQUILIBRIUM EQUATIONS

The basic principle involved in the application of the fundamental equations (21) and (22) to the treatment of a practical problem is that the equilibrium state of the tilt field  $\mathbf{d}$  as well as  $\mathbf{Y}$  is always given by minimizing the total free energy of the system. In order to obtain the tilt and surface-equilibrium equations one has to derive the Euler-Lagrange differential equations by calculating the variation of the free energy. By using Eq. (21) and noting that  $dA = \sqrt{g} du dv$ , we can write the variation as

$$\delta F = \delta \int \sqrt{g} g_{\text{TCLB}} du dv . \quad (23)$$

The Euler-Lagrange equations from variation of functions  $d_i$  ( $i = 1, 2$ ) are given by

$$\left[ \frac{\partial}{\partial d_i} - \partial_j \frac{\partial}{\partial d_{i,j}} \right] \sqrt{g} g_{\text{TCLB}} = 0 . \quad (24)$$

Inserting Eq. (22) into Eq. (24) yields

$$2\lambda \sqrt{g} g_{ij} d_j + k_2 t \epsilon_{3jk} [2 \cos \theta_0 (g_{kl} L_{ij} + g_{ik} L_{jl}) d_l - \cos^2 \theta_0 (g_{kl} \Gamma_{ij}^l + g_{ij,k})] = 0 \quad (i = 1, 2) . \quad (25)$$

This is the equation we are looking for. If the surface  $\mathbf{Y}(u, v)$  is given, one can completely determine  $d_1(u, v)$ ,  $d_2(u, v)$ , and  $\lambda(u, v)$  by solving Eqs. (5) and (25). Hence we call Eq. (25) the tilt-equilibrium equation.

To derive the surface-equilibrium equation one has to calculate the part of  $\delta F$  that comes from the shape variation. We assume  $\mathbf{Y}(u, v)$  is the equilibrium shape and consider a slightly distorted surface defined by

$$\mathbf{Y}'(u, v) = \mathbf{Y}(u, v) + \psi(u, v) \mathbf{n} , \quad (26)$$

where  $\psi$  is a sufficiently small and smooth function of  $u, v$ . The variation of free energy caused by  $\psi$  then reads as

$$\delta F = F(\mathbf{Y}') - F(\mathbf{Y}) . \quad (27)$$

After tedious algebraic manipulations by using the relations derived in Ref. 19, correct to the first-order quantity of  $\psi$ , we found that

$$\delta F = \int \left[ \frac{2}{\sqrt{g}} \cos \theta_0 k_2 t \epsilon_{3ji} \times [(Kg_{jk} - 2HL_{jk}) + (\partial_j \partial_k + \partial_m \Gamma_{jk}^m)] g_{il} d_k d_l - 2\lambda L_{ij} d_i d_j \right] \psi dA, \quad (28)$$

where  $H$  and  $K$  are the mean curvature and Gaussian curvature of the surface defined as

$$H = \frac{1}{2} g^{ij} L_{ij}, \quad K = L/g, \quad L = \det(L_{ij}). \quad (29)$$

Since  $\mathbf{Y}(u, v)$  is assumed as an equilibrium shape, it satisfies the condition  $\delta F = 0$  for any  $\psi(u, v)$ , which leads Eq. (28) to the surface-equilibrium condition

$$\frac{2}{\sqrt{g}} k_2 t \cos \theta_0 \epsilon_{3ji} [(Kg_{jk} - 2HL_{jk}) + (\partial_j \partial_k + \partial_m \Gamma_{jk}^m)] g_{il} d_k d_l - 2\lambda L_{ij} d_i d_j = 0. \quad (30)$$

With the algebraic equations (5) and (25) for  $\lambda$  and  $d_i$  ( $i=1, 2$ ),  $\lambda$  and  $d_i$  can be completely expressed by the differential geometry quantities  $g_{ij}$ ,  $L_{ij}$ , and  $\Gamma_{ij}^k$  of surface  $\mathbf{Y}(u, v)$ . Substituting them into Eq. (30) will give a full form of the surface-equilibrium equation in which  $d_i$  and  $\lambda$  disappear. However, this form of the equation is quite involved, so instead we will use Eqs. (5), (25), and (30) together for analysis of practical problems in the following sections.

The surface-equilibrium equation (30), from the view of physics, represents the balance of normal force per unit area of the surface while the tilt-equilibrium equation (25) describes the balance of the moments of force under condition (5). Both of them contain terms of complicated stresses and torsions of curvature elasticity, respectively. It is the torsion that induces the twist of the TCLB and gives rise to the helical structures, as shown in the following sections.

#### IV. APPLICATION TO HELICAL STRUCTURES AND SPHERE

##### A. Wound-ribbon helix

Figure 2 shows a ribbon wound around a cylinder with radius  $\rho_0$ . In cylindrical coordinates,  $u = \phi$ ,  $v = z$ , the cylindrical surface is described by

$$\mathbf{Y} = (\rho_0 \cos \phi, \rho_0 \sin \phi, z). \quad (31)$$

The fundamental quantities associated with this surface have been obtained<sup>19</sup> as

$$\begin{aligned} g_{11} &= \rho_0^2, \quad g_{12} = g_{21} = 0, \quad g_{22} = 1, \\ \mathbf{n} &= (\cos \phi, \sin \phi, 0), \quad \Gamma_{ij}^k = 0, \\ H &= -\frac{1}{2} \rho_0, \quad K = 0, \\ KL^{11} &= KL^{12} = KL^{21} = 0, \quad KL^{22} = -\frac{1}{\rho_0}. \end{aligned} \quad (32)$$

Substituting Eq. (32) into Eqs. (5) and (25) one has

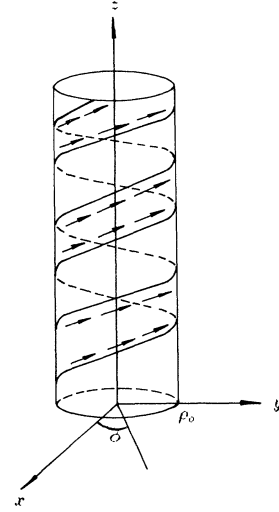


FIG. 2. Schematic illustrations of the wound-ribbon helix. The arrows represent the local tilt direction.

$$\rho_0^2 d_1^2 + d_2^2 - \sin^2 \theta_0 = 0 \quad (33)$$

and

$$-k_2 t \cos \theta_0 d_2 + \lambda \rho_0^2 d_1 = 0, \quad (34)$$

$$-k_2 t \cos \theta_0 d_1 + \lambda d_2 = 0. \quad (35)$$

Solving Eqs. (33)–(35), one finds

$$\begin{aligned} d_1 &= \alpha_1 \frac{\sin \theta_0}{\sqrt{2} \rho_0}, \\ d_2 &= \alpha_2 \frac{\sin \theta_0}{\sqrt{2}}, \\ \lambda &= \frac{\alpha_1 k_2 t}{\alpha_2 \rho_0} \cos \theta_0, \end{aligned} \quad (36)$$

where  $(\alpha_1, \alpha_2) = (\pm 1, \pm 1)$  or  $(\pm 1, \mp 1)$  depending on the sign of  $k_2$ . The orientation field  $\mathbf{d}$  is given by Eqs. (4), (31), and (36) as

$$\mathbf{d} = \frac{\alpha_1 \sin \theta_0}{\sqrt{2}} (-\sin \phi, \cos \phi, 0) + \frac{\alpha_2 \sin \theta_0}{\sqrt{2}} (0, 0, 1) + \cos \theta_0 \mathbf{n}. \quad (37)$$

Equation (37) reveals that the local azimuthal angle of the director must be  $45^\circ$  or  $-135^\circ$  for  $(\alpha_1, \alpha_2) = (\pm 1, \pm 1)$ ,  $-45^\circ$  or  $135^\circ$  for  $(\alpha_1, \alpha_2) = (\pm 1, \mp 1)$ . Compare this theoretical result with experiments in which it is observed that the gradient angle  $\varphi$  of the wound-ribbon edge is always near  $\pm 45^\circ$ , it indicates that the edge line of the ribbon is parallel to the azimuthal direction of the director. This choice is consistent with the assumption taken by Helfrich.<sup>14</sup>

The question that remains to be answered is how to determine the sign of  $\varphi$ ? To answer this question one has to calculate the free energy of the ribbon with an arbitrary winding sense, the correct winding sense should correspond to the configuration with lower free energy.

By using Eqs. (32) and (36) one obtains from Eqs. (21) and (22)

$$F_W = -\frac{2\alpha_1\alpha_2k_2At\cos\theta_0\sin^2\theta_0}{\rho_0}, \quad (38)$$

where  $A$  is the total area of the ribbon. Since the titled angle  $\theta_0$  is defined as an acute angle, from Eq. (38) one immediately sees that the right-handed helix ( $\alpha_1\alpha_2=1$ ) has lower free energy than the left-handed helix ( $\alpha_1\alpha_2=-1$ ) whenever  $k_2>0$ , and  $k_2<0$  will be favored to form the left-handed helix. This result agrees with cholesteric liquid crystals in which  $k_2>0$  and  $k_2<0$  corresponds to the right-hand and left-hand twist patterns, respectively.

Finally, one should test whether these cylindrical ribbons satisfy the surface-equilibrium equation (30). With Eq. (32) and the fact that both  $d_1$  and  $d_2$  are constants, one finds that equation (30) is reduced to

$$k_2t\cos\theta_0d_1d_2-\lambda\rho_0^2d_1^2=0, \quad (39)$$

which is identical to Eq. (34). Therefore, the results obtained in this section indicate that the experimentally observed wound-ribbon helices do satisfy exactly the tilt-equilibrium and surface-equilibrium equations derived in Sec. III.

### B. Twisted strip

In this section we will treat the second-type helical structure of the TCLB, the twisted strips, which, to our knowledge, has not been theoretically treated yet.

The geometry of this type of helical structure is shown in Fig. 3; analytically we choose a helicoid to represent it. In polar coordinates the helicoid is described as

$$\mathbf{Y}=(\rho\cos\phi,\rho\sin\phi,b\phi), \quad (40)$$

where  $|\rho|\leq R$ ,  $R$  is the radius of the helicoid,  $0\leq\phi\leq 2n\pi$ , and  $n$  is the spiraling number. The constant parameter  $b$  characterizes the parity of the twisted strip, e.g., a positive  $b$  represents a right-hand twisted strip and a negative  $b$  represents a left-hand one;  $2\pi|b|$  is the pitch of the helix.

With  $u=\rho$  and  $v=\phi$ , a straightforward calculation gives

$$\mathbf{Y}_1=(\cos\phi,\sin\phi,0), \quad \mathbf{Y}_2=(-\rho\sin\phi,\rho\cos\phi,b), \quad (41)$$

$$\mathbf{n}=\frac{(b\sin\phi,-b\cos\phi,\rho)}{(\rho^2+b^2)^{1/2}}, \quad (42)$$

$$g_{11}=1, \quad g_{12}=g_{21}=0, \quad g_{22}=g=\rho^2+b^2, \\ L_{11}=0, \quad L_{12}=L_{21}=-\frac{b}{(\rho^2+b^2)^{1/2}}, \quad L_{22}=0, \quad (43)$$

$$H=0, \quad K=-\frac{b^2}{(\rho^2+b^2)^{1/2}},$$

$$\Gamma_{12}^2=\Gamma_{21}^2=\frac{\rho}{\rho^2+b^2}, \quad \Gamma_{22}^1=-\rho.$$

The other Christoffel symbols are zero. In terms of the above given quantities, Eqs. (5) and (25) become

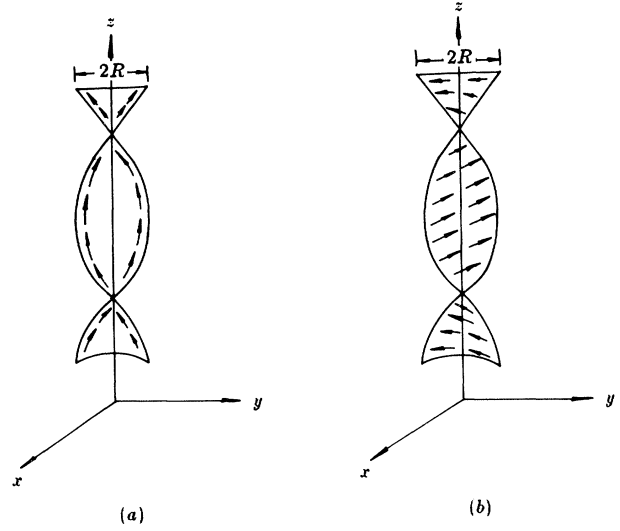


FIG. 3. Schematic illustrations of the twisted strip helix. (a) The tilt field corresponds to Eq. (47). (b) The tilt field corresponds to Eq. (48). The arrows represent the local tilt direction.

$$d_1^2+(\rho^2+b^2)d_2^2-\sin^2\theta_0=0, \quad (44)$$

$$d_1[k_2tb\cos\theta_0+\lambda(\rho^2+b^2)]=0, \quad (45)$$

$$d_2[2k_2tb\cos\theta_0-\lambda(\rho^2+b^2)]=0. \quad (46)$$

Two sets of solutions for  $d_1$ ,  $d_2$ , and  $\lambda$  are obtained from Eqs. (44)–(46) as

$$d_1=0, \\ d_2=\pm\frac{\sin\theta_0}{(\rho^2+b^2)^{1/2}}, \quad (47) \\ \lambda=\frac{2k_2tb\cos\theta_0}{\rho^2+b^2},$$

and

$$d_1=\pm\sin\theta_0, \\ d_2=0, \quad (48) \\ \lambda=-\frac{k_2tb\cos\theta_0}{\rho^2+b^2}.$$

The fields of azimuthal angle  $\phi$  corresponding to Eqs. (47) and (48) are schematically illustrated in Figs. 3(a) and 3(b), respectively. These figures clearly show that for the first kind of twisted strip represented by Eq. (47), the orientation is along the edge line [Fig. 3(a)], while for the second kind represented by Eq. (48), the orientation of the director is perpendicular to the edge line [Fig. 3(b)].

One can easily verify that the surface-equilibrium equation is satisfied by both kinds of twisted strips given above. Substituting Eqs. (41)–(43) into Eq. (30) yields

$$\{k_2t\cos\theta_0[\partial_\rho^2(\rho^2+b^2)-\rho\partial_\rho+\partial_\phi^2]+2\lambda b\}d_1d_2=0. \quad (49)$$

There is no need of further derivation; one can see that this equation is automatically satisfied by  $d_1$ ,  $d_2$ , and  $\lambda$

given in Eqs. (47) and (48).

The calculation of free energy for both kinds of twisted strips is rather involved; the final results are

$$F_T^{(1)} = -F_T^{(2)} = -\frac{2k_2 A t \cos\theta_0 \sin^2\theta_0 f(R/b)}{R}, \quad (50)$$

where  $F_T^{(1)}$  and  $F_T^{(2)}$  denote the free energy of twisted strips corresponding to Eqs. (47) and (48), respectively,  $A$  is the total area of the twisted strip, and  $f(R/b)$  is a function of  $R/b$  with a rather complicated form as

$$f(x) = 2x \frac{\ln[x + (1+x^2)^{1/2}]}{x(1+x^2)^{1/2} + \ln[x + (1+x^2)^{1/2}]}. \quad (51)$$

It is interesting to note that if one puts  $R = \rho_0$ , then the expression of free energy of twisted strips  $F_T^{(1)}$  is similar to that of the wound-ribbon helix given by Eq. (38) apart from a factor  $f(\rho_0/b)$ . From the expression for  $F_T^{(1)}$  and Eq. (51) one sees that for  $k_2 > 0$ , the right-hand twisted strip ( $b > 0$ ) has lower free energy than the left-hand one ( $b < 0$ ), while for  $k_2 < 0$ , the left-hand twisted strip is energy favorable state. This conclusion is consistent with what we got for the wound-ribbon helix and, of course, with the property of the cholesteric liquid crystals.

However, using the same analysis for the expression of  $F_T^{(2)}$  for the second kind of twisted step represented by Eq. (48), the situation is just reversed. According to the general point of view,<sup>21</sup> the sign of  $k_2$  should be determined by the chirality of the molecules. Therefore, this analysis provides an interesting structure which shows that the helical senses of macrostructure are not always coincident with the microscopic chiral senses of the composed molecules. Whether this kind of structure is only an unphysical solution of the equation or it has some significance in biological genetics depends on further experimental investigation.

In order to discuss the transition between the wound-ribbon helix and the twisted strip, one has to evaluate the values of factor function  $f(R/b)$  for given  $R/b$ . Numerical analysis shows that

$$|f(R/b)| \leq 0.984, \quad (52)$$

and  $|f(x)|$  takes its maximum at

$$\frac{R}{|b|} = 2.34. \quad (53)$$

Comparing Eq. (38) to Eq. (50) indicates that for a same strip of the TCLB (i.e.,  $A = A$ ,  $\rho_0 = R$ ), the wound-ribbon helix always has lower free energy than the twisted strip does, regardless of which type of twisted strip the latter belongs to. This, at least it seems to us, explains the spontaneous transition from the twisted strip to the wound-ribbon observed in experiments [see Figs. 1(A)–1(D) of Ref. 5].

### C. Spherical vesicle

Some experimental studies<sup>5,7</sup> observed that before the growth of the helical structure from fibrous bilayers, the chiral bilayers may close to form spherical vesicles. Therefore there are some interests to calculate the orien-

tation field of the chiral molecules on a spherical surface.

In spherical polar coordinates,  $u = \theta$ ,  $v = \phi$ , the spherical surface with radius  $r_0$  is denoted by

$$\mathbf{Y} = r_0(\cos\phi \sin\theta, \sin\phi \sin\theta, \cos\theta). \quad (54)$$

The basic differential geometric quantities of a spherical surface with radius  $r_0$  are

$$\begin{aligned} g_{11} &= r_0^2, & g_{12} &= g_{21} = 0, & g_{22} &= r_0^2 \sin^2\theta, \\ L_{11} &= -r_0, & L_{12} &= L_{21} = 0, & L_{22} &= r_0 \sin^2\theta, \\ H &= -\frac{1}{r_0}, & K &= \frac{1}{r_0^2}, \end{aligned} \quad (55)$$

$$\begin{aligned} \Gamma_{11}^1 &= \Gamma_{11}^2 = \Gamma_{12}^1 = \Gamma_{22}^2 = 0, & \sin^2\theta \Gamma_{12}^2 &= -\Gamma_{22}^1 \\ & & &= \sin\theta \cos\theta. \end{aligned}$$

With these quantities going through procedures similar to Secs. IV A, and IV B, we obtained the equations which determine  $d_1$ ,  $d_2$ , and  $\lambda$  as

$$d_1^2 + \sin^2\theta d_2^2 - \frac{\sin^2\theta_0}{r_0^2} = 0, \quad (56)$$

$$\lambda \sin\theta d_1 = 0, \quad (57)$$

$$\lambda \sin^2\theta d_2 = 0. \quad (58)$$

Two sets of apparent solutions of Eqs. (56)–(58) are

$$\begin{aligned} d_1 &= 0, \\ d_2 &= \pm \frac{\sin\theta_0}{r_0 \sin\theta}, \\ \lambda &= 0, \end{aligned} \quad (59)$$

and

$$\begin{aligned} d_1 &= \pm \frac{\sin\theta_0}{r_0}, \\ d_2 &= 0, \\ \lambda &= 0. \end{aligned} \quad (60)$$

With both solutions (59) and (60) it is readily shown that such a spherical surface satisfies the surface-equilibrium equation (30). The azimuthal angle fields of the tilted director corresponding to both sets of solutions are sketched in Figs. 4(a) and 4(b) as latitudinal lines and longitudinal lines on the spherical surface, respectively. In both cases, the orientation of the director is found being discontinuous at the north pole and the south pole. This is by no means a surprise but a natural consequence of the theorem of differential geometry which states that on a closed surface of topological sphere a line field has at least two singular points.<sup>22</sup> Of course, from Eqs. (56)–(58) one can find more solutions of  $d_1, d_2$  in which  $\lambda$  has to be zero. As an example, Fig. 4(c) shows one of these solutions which is a proper combination of latitudinal and longitudinal lines. It is worthy to point out that this kind of fields has more points of singularity.

The above given analysis clearly shows that for the

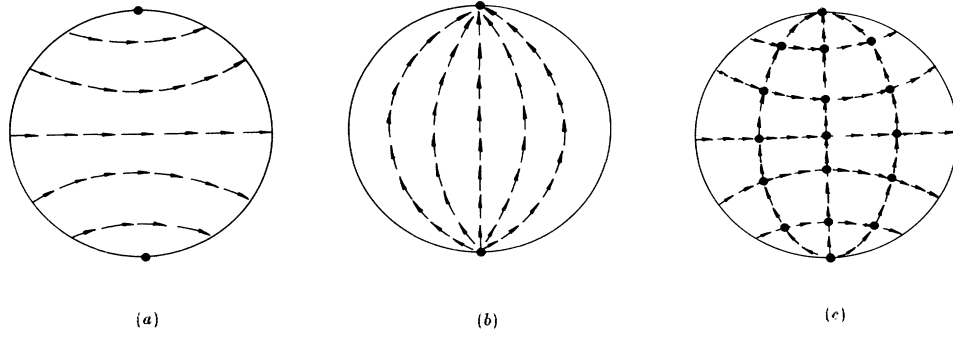


FIG. 4. Schematic illustrations of spherical vesicles. (a) The tilt field corresponds to Eq. (59). (b) The tilt field corresponds to Eq. (60). (c) The tilt field corresponds to one of the other solutions of Eqs. (56)–(59). The arrows represent the local tilt direction.

field of the TCLB vesicle there are at least two defects (singular points). If one assumes that these defects will cause the leakage and fusion of vesicles, then the feature of the orientation field in a spherical surface given above provides a rather reasonable explanation for the experimentally observed fact of transition from vesicular dispersion to helical superstructure formation of the TCLB [Figs. 1(A)–1(D) of Ref. 5].

In their experiment,<sup>5</sup> Nakashima *et al.* observed that with the decrease of temperature, there is a transition process from vesicle-to-vesicle fusion, and finally to the formation of aggregated helical structures. From our point of view, this process may be conceived as a consequence of a transition from the  $L_\alpha$  phase of the bilayer material (at this phase a vesicle has no tilt and defect of orientation) to the  $L_{\beta^*}$  phase. At the latter phase, according to this theory, the tilt of molecules will cause the orientation defects which may lead to the vesicle fusion and the formation of helical structures.

In general, the transition from vesicle to helical structures can be seen from the energy point of view.

Using Eqs. (55), (59), and (60) one can calculate the free energy of a vesicle from Eqs. (21) and (22) with condition  $\lambda=0$  as

$$\begin{aligned}
 F_S^{\text{longitud}} &= -k_2 t \cos^2 \theta_0 \int \int (g_{22} d_{2,1} + g_{22} \Gamma_{12}^2 d_2) d\theta d\phi \\
 &= -k_2 t \cos^2 \theta_0 \int \int d\theta d\phi (r_0^2 \sin^2 \theta) \left[ -r_0^{-1} \sin \theta_0 \frac{\cos \theta}{\sin^2 \theta} + r_0^{-1} \sin \theta_0 \sin \theta^{-1} \frac{\cos \theta}{\sin \theta} \right] \\
 &= 0.
 \end{aligned} \tag{64}$$

Therefore, for both tilt fields of vesicle the final result is

$$F_S = F_S^{\text{longitud}} = F_S^{\text{latitud}} = 0. \tag{65}$$

Comparing Eqs. (38), (50), and (52) with (65), there is a free-energy sequence

$$F_S > F_T > F_W, \tag{66}$$

which confirms the observed transition from vesicular dispersion to twisted strips and wound ribbon. Figure 5

$$\begin{aligned}
 F_S &= -k_2 t \cos \theta_0 \\
 &\quad \times \int \int \epsilon_{3jm} [\cos \theta_0 (g_{mk} d_{k,j} + g_{ml} \Gamma_{jk}^l d_k) \\
 &\quad \quad - 2L_{jk} g_{ml} d_k d_l] d\theta d\phi,
 \end{aligned} \tag{61}$$

where the intervals of integration for  $\theta$  and  $\phi$  are  $[0, \pi]$  and  $[0, 2\pi]$ , respectively. Since for  $\epsilon_{3jm}$  only  $(j, m) = (1, 2)$  has to be considered ( $\epsilon_{321} = -1$ ,  $\epsilon_{312} = 1$ ) and  $g_{km}$  is a diagonal tensor,

$$\begin{aligned}
 F_S &= -k_2 t \cos \theta_0 \int \int [\cos \theta_0 (g_{22} d_{2,1} + g_{22} \Gamma_{12}^2 d_2 \\
 &\quad - g_{11} d_{1,2} - g_{11} \Gamma_{22}^1 d_1) \\
 &\quad - 2(L_{11} g_{22} d_1 d_2 - L_{22} d_1 d_2 \\
 &\quad - L_{22} g_{11} d_2 d_1)] d\theta d\phi.
 \end{aligned} \tag{62}$$

Substituting the latitudinal tilt field given by Eq. (59) to Eq. (62), one has

$$\begin{aligned}
 F_S^{\text{latitud}} &= k_2 t \cos^2 \theta_0 \int \int g_{11} \Gamma_{22}^1 d_1 d\theta d\phi \\
 &= -k_2 t \cos^2 \theta_0 \sin \theta_0 r_0 \int_0^{2\pi} d\phi \int_0^\pi \sin \theta \cos \theta d\theta \\
 &= 0.
 \end{aligned} \tag{63}$$

Similarly, for the latitudinal tilt field given by Eq. (60).

illustrates this transition sequence of different shapes of the membrane. Consider the conventional choice that the local tilt direction should be along the edge line of the helical structure; the second kind of twisted strip illustrated in Fig. 3(b) is ruled out from this sequence.

#### D. A general formula of free energy of the TCLB

To compare with other theories, in this section a general formula for the free energy of the TCLB in the form

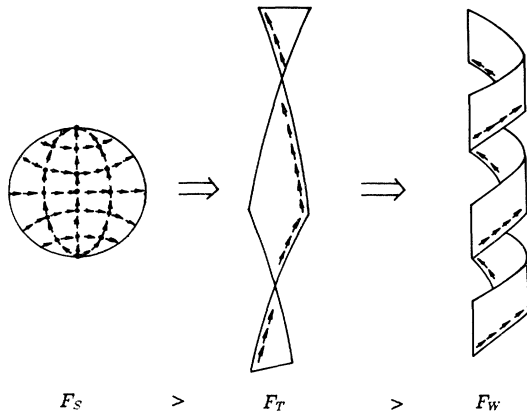


FIG. 5. Schematic illustration of the transition sequence from the vesicle to helical structure. The arrows represent the local tilt direction.

of differential geometry is given and its derivation is presented. This formula, as shown later, may explain the formation of a prolate tube from the wound-ribbon helix on a straight cylinder.

As shown in Secs. IV A–IV C, the free energy of the TCLB depends only on the project field on the TCLB surface casted by  $\mathbf{d}$  apart from some constant factors of  $\theta_0$ . Hence it should be possible to express the energy with some basic geometry quantities associated with this project line field. From Eq. (4), the project line field is nothing but  $d_i Y_i$ . So we consider now the single infinite family of curves on the surface  $\mathbf{Y}(u, v)$ , denoting  $\mathbf{Y}(l) = \mathbf{Y}(u(l), v(l))$  and taking  $d\mathbf{l}$  along the direction  $d_i Y_i$ , then the unit tangent at any point of the curve in the family may be written as

$$\dot{\mathbf{Y}} = \frac{d\mathbf{Y}}{dl} = \mathbf{Y}_i \frac{du^i}{dl} = \mathbf{Y}_i d_i / \sin\theta_0, \quad (67)$$

and, similarly, one has

$$\dot{\mathbf{n}} = \frac{d\mathbf{n}}{dl} = \mathbf{n}_i d_i / \sin\theta_0 = -L_{ij} g^{jk} \mathbf{Y}_k d_i / \sin\theta_0. \quad (68)$$

The last equation is followed from the Weingarten theorem.<sup>22</sup> The geodesic torsion of the local tilt field  $\tau_g$  then may be calculated as

$$\begin{aligned} \tau_g &= \dot{\mathbf{n}} \cdot (\mathbf{Y} \times \mathbf{n}) \\ &= -L_{ij} g^{jk} \mathbf{Y}_k \cdot (\mathbf{Y}_m \times \mathbf{n}) d_i d_m / \sin^2\theta_0. \end{aligned} \quad (69)$$

Due to  $\mathbf{Y}_k \times \mathbf{Y}_m = \epsilon_{3km} \sqrt{g} \mathbf{n}$ , Eq. (69) can be rewritten as

$$\tau_g = -\epsilon_{3km} g^{jk} L_{ij} \sqrt{g} d_i d_m / \sin^2\theta_0. \quad (70)$$

Using the identity

$$\epsilon_{3km} g^{jk} = \frac{1}{g} \epsilon_{3jk} g_{km}, \quad (71)$$

Eq. (70) is changed to

$$\tau_g = \epsilon_{3jk} g_{km} L_{ij} d_i d_m / \sin^2\theta_0 \sqrt{g}. \quad (72)$$

The other quantity needs to be calculated is the following integral:

$$\sigma \equiv \int \epsilon_{3ji} (g_{ik} d_{k,j} + g_{ii} \Gamma_{kj}^l d_k) du^1 du^2. \quad (73)$$

With the definition of  $\Gamma_{kj}^l$  we have

$$\sigma = \int \epsilon_{3ji} [g_{ik} d_{k,j} - \frac{1}{2} (g_{kj,i} - g_{ki,j} - g_{ji,k}) d_k] du^1 du^2 \quad (74)$$

or

$$\sigma = \int \epsilon_{3ji} [\partial_j (g_{ik} d_k) - \frac{1}{2} (g_{kj,i} + g_{ki,j} - g_{ji,k})] du^1 du^2. \quad (75)$$

Noticing that  $\epsilon_{3ji} = -\epsilon_{3ij}$  and  $g_{lm} = g_{ml}$ , it is easy to see that

$$\epsilon_{3ji} (g_{kj,i} + g_{ki,j}) = 0 \quad (76)$$

and

$$\epsilon_{3ji} g_{ji,k} = 0. \quad (77)$$

Hence we have

$$\sigma = \int \epsilon_{3ji} \partial_j (g_{ik} d_k) du^1 du^2. \quad (78)$$

By using Green's theorem, Eq. (78) can be written as a line integral

$$\sigma = \oint g_{ik} d_k du^i = \oint (\mathbf{Y}_i \cdot \mathbf{Y}_k) d_k du^i = \oint \mathbf{d} \cdot d\mathbf{l}, \quad (79)$$

where  $\mathbf{d} = \mathbf{Y}_k d_k + \mathbf{n} \cos\theta_0$  is of the same definition as Eq. (4), and  $d\mathbf{l} = \mathbf{Y}_i du^i$  is the line element of the edge line of the TCLB. Substituting Eqs. (72) and (73) [i.e., (79)] into Eqs. (21) and (22) one obtains the general expression

$$\begin{aligned} F = \int g_{\text{TCLB}} dA &= -k_2 t \cos^2\theta_0 \oint \mathbf{d} \cdot d\mathbf{l} - 2k_2 \sin^2\theta_0 \cos\theta_0 \\ &\quad \times \int \tau_g dA. \end{aligned} \quad (80)$$

If one sets  $\theta_0 = 0$ , which corresponds to fluid membranes and  $\mathbf{d} \perp d\mathbf{l}$ , then Eq. (80) gives  $F = 0$ . This means that the effect of the chiral curvature elasticity can be displayed only when there is the tilt of the director.

It is well known that<sup>22</sup> the geodesic torsion  $\tau_g$  may be expressed as

$$\tau_g = (c_1 - c_2) \sin\varphi \cos\varphi, \quad (81)$$

where  $c_1$  and  $c_2$  are the two principal curvatures and  $\varphi$  is the angle between one principle direction and the local tilt direction. The angular dependence is just what Helfrich and Prost<sup>16</sup> found in the  $S_c^*$  model for the wound-ribbon helix. However, the line-integral term did not appear in their work; it appears here for the first time and has some important consequences. For half of the sphere illustrated in Fig. 4(b), it implies a negative-edge energy if  $k_2$  corresponds to the appropriate rotational sense. To apply Eq. (81) to the wound-ribbon helix structure discussed in Sec. IV A is interesting. Since for the cylindrical surface  $c_1 = 0$ ,  $c_2 = -1/2\rho_0$ , the corresponding Eq. (81) becomes

$$\tau_g = \frac{1}{2\rho_0} \sin\varphi \cos\varphi, \quad (82)$$

which immediately gives that for the wound-ribbon helix, since the first term of Eq. (80) is zero, the minimum of free energy of the structure is reached at

$$\varphi = \pm 45^\circ \quad (83)$$

for  $k_2 > 0$  and  $k_2 < 0$ , respectively. This result is in agreement with what we obtained in Sec. IV A.

## V. TUBE RADIUS AND HELICAL PITCH

In previous sections, by only keeping the chiral terms in the Frank expression of elastic free energy we discussed the helical structures of the TCLB and obtained fairly satisfactory explanations of the transition from the vesicle to the formation of the helical superstructure observed in experiments. This encouraging result shows that the cholesteric tilt of the director indeed plays a crucial role in the formation of helical structures of the TCLB. As we mentioned in Sec. II, after the effect of the chiral term is investigated and a rather successful understanding of this term is obtained, we now turn back to include other terms of the full expression of Frank free energy for consideration. We expect by doing this the effects from other curvature energy terms can be revealed and the problem can be understood deeper.

In the complete expression of Frank free energy for cholesteric liquid crystal, the part of the curvature energy density terms which satisfies  $D_{\infty h}$  symmetry

$$g_N = \frac{1}{2} [k_{11} (\nabla \cdot \mathbf{d})^2 + k_{22} [\mathbf{d} \cdot (\nabla \times \mathbf{d})]^2 + k_{33} (\mathbf{d} \times \nabla \times \mathbf{d})^2] \quad (84)$$

should be considered together with the chirality term of free-energy density  $g_{\text{ch}}$  given in Eq. (6), where  $k_{11}$ ,  $k_{22}$ , and  $k_{33}$  are the splay, twist, and bend elastic constants. Therefore, we naturally add this part of the energy density to  $g_{\text{ch}}$  for consideration. Since Eq. (84) is the full expression of the free-energy density for nematics ( $N$ ), we denote it by  $g_N$ . Before getting into practical calculations we simplify the expression of Eq. (84) by assuming  $k_{11} = k_{22} = k_{33} = k_N$ . By doing this the mathematical manipulations following are greatly simplified but, as shown latter, the general behavior of the result is not affected. After some algebraic manipulations, one has

$$g_N = \frac{k_N}{2} [(\nabla \cdot \mathbf{d})^2 + (\nabla \times \mathbf{d})^2]. \quad (85)$$

To express the formula to a curved surface the second term on the right-hand side of the equation should be treated as for Eq. (17), while the first term can be transformed by taking<sup>20</sup>

$$\nabla \cdot \mathbf{d} = d_{i,i} + \Gamma_{ij}^j d_i - 2H \cos\theta_0. \quad (86)$$

Using these and the other relevant formulas derived in Sec. IV, the additional free-energy density for a wound-ribbon helix is calculated and the result is

$$\begin{aligned} F_N &= \int g_N dV \\ &= t \cos\theta_0 \int g_N dA \\ &= \frac{1}{2} k_N A t (1 + \sin^2\theta_0) \cos\theta_0 / \rho_0^2. \end{aligned} \quad (87)$$

The total free-energy density for the wound-ribbon helix then is

$$\begin{aligned} F_{WT} &= F_N + F_W \\ &= A \left[ \frac{k_N t}{2\rho_0^2} (1 + \sin^2\theta_0) - \frac{2|k_2|t}{\rho_0} \sin^2\theta_0 \right] \cos\theta_0, \end{aligned} \quad (88)$$

where we have set  $\alpha_1 \alpha_2 k_2 = |k_2|$ .

It is interesting to see that in the expression of free energy (88) two terms are competing with each other. For lowering the free energy, the first term, i.e., the nematic term, tends to increase  $\rho_0$  while the second term representing the chiral effect tends to reduce  $\rho_0$ . It is this competition between two effects that determines the size of the helical structure  $\rho_0$ . The minimization of Eq. (82) with respect to  $\rho_0$  yields

$$\rho_0 = \frac{k_N}{2|k_2|} \frac{(1 + \sin^2\theta_0)}{\sin^2\theta_0}, \quad (89)$$

where the ratio  $k_N/|k_2|$  is nothing but  $p_{\text{ch}}/\pi$ ,  $p_{\text{ch}}$  being the pitch of cholesterics.<sup>21</sup> Hence we find the tube radius of the wound-ribbon helix is

$$\rho_0 = \frac{p_{\text{ch}}}{2\pi} \frac{1 + \sin^2\theta_0}{\sin^2\theta_0}. \quad (90)$$

Considering the fact that the gradient angle is  $\pm 45^\circ$ , the pitch of the wound-ribbon helix is given by

$$p = 2\pi\rho_0 = p_{\text{ch}} \frac{1 + \sin^2\theta_0}{\sin^2\theta_0}. \quad (91)$$

These last two expressions clearly demonstrated the effects of chirality ( $p_{\text{ch}}$ ) and director tilt ( $\theta_0$ ) on the formation of helical structures and tubes. Since, if one takes the limit cases of setting either  $\theta_0 = 0$  or  $p_{\text{ch}} = \infty$ , then from Eqs. (89)–(91),  $\rho_0, p \rightarrow \infty$ , which means that there is no formation of the tube and helix at all.

Equations (89)–(91) numerically provide the size of the tube and helix. Due to the fact that for usual cholesterics  $p_{\text{ch}} = 0.1 \sim 100 \mu\text{m}$ , then from Eqs. (89)–(91) one immediately concludes that the radius of the tube and the helix pitch are of the order of magnitude  $0.1 \sim 100 \mu\text{m}$ . This is in agreement with experimental observations.<sup>5–11</sup> For instance, at a temperature near the formation temperature of helical structure  $T_c$ , Nakashima and co-workers<sup>7</sup> observed that the pitch of a long helix of  $2C_{12}\text{-L-Glu-C}_{11}\text{N}^+$  is about  $3 \mu\text{m}$ .

Careful readers may already notice the difference between expressions (87)–(91) and the corresponding expressions in Ref. 4; it comes from different definitions of the thickness of the layer in two papers. The similar calculations show that for twisted strips both  $\rho_0$  and  $p$  also have the same order of magnitude, the difference is only a factor close to unity.

Besides giving the size of helical structures by Eqs. (89)–(91), Eqs. (87) and (88) indicate that, as the area  $A$  increases, the total free energy  $F_{WT}$  becomes more negative. This may explain the formation of prolate tube and multilamellar aggregation.

## VI. CONCLUSIONS

In this work, a theory of tilted cholesteric lipid bilayers is developed and the application of the theory to helical structures of the TCLB is presented. The results obtained show that even only taking the chiral term of the curvature terms in the Frank theory of cholesteric liquid crystals into consideration, the transition from vesicular dispersion to the formation of two types of helical superstructure of the TCLB is elucidated in good agreement with experimental observations. This may imply that the basic idea of the theory hits the key point of the mechanism behind the phenomena in discussion. From the calculations of free energy and equilibrium equations for both direction orientation and the surface several conclusions can be drawn as follows.

Firstly, the orientation field of a TCLB vesicle has to involve more than two points of singularity; these defects may cause the dispersion of the vesicle. In other words, the  $L_\alpha$  to  $L_{\beta^*}$  transition can induce the fission of the membrane vesicle. This effect may have some physiological significance.

Secondly, although the spherical vesicle, the twisted strip, and the wound-ribbon helix with some appreciated orientation fields, respectively, are observed in experiments and satisfy the equilibrium equations derived in this work, these three states of the TCLB propose a sequence from higher free energy to a lower one. This sequence of free energy indicates a correct transition direction of the states of the TCLB observed in experiments.

Thirdly, as we have shown in the calculations, the helical senses for both the wound-ribbon helix (with the assumption that the local direction of the tilt along the

edge line) and the first kind of twisted strip coincide with the cholesteric liquid crystal, i.e., the molecular chirality. And, all the experimentally observed helical structures reported up to now support this result. However, for the second kind of twisted strip, and the wound-ribbon structure obtained under the assumption that the local tilt direction is perpendicular to the edge line of the ribbon, this principle fails to apply. At this stage, though these structures are not observed in experiment, it seems worthy to note these structures to biological geneticists. Whether they are only unphysical solutions of the equations derived in this work or they may relate with some anomalies in biology is an open question.

Finally, we would like to stress that the theory presented in this work is based on the assumption that the chiral effect is much stronger than the effects of other terms in the Frank free-energy expression, and the calculation carried out for the helical structures of the TCLB is started from the variation of the chiral term of elasticity free energy. Though quite reasonable results were obtained to apply this theory to helical structures observed in experiments, the calculation in Sec. V apparently shows that including other terms in elasticity free energy is important. Therefore, to thoroughly understand the helical structures, a more complete theory which may consider both the chiral effect and other effects is urgently needed. In this sense the present work may be considered as the first step of the new theory.

## ACKNOWLEDGMENTS

This work is partially supported by The National Natural Science Foundation of China. The authors would like to thank Professor W. Helfrich for the stimulating discussion at the beginning of this work; the idea of the cholesteric liquid-crystal approach adopted in this work has come from his paper on helical structure (Ref. 14). We also thank Professor M. Wortis for his critical reading of the preliminary manuscript.

<sup>1</sup>W. Helfrich, *Naturforsch.* **28**, 693 (1973).

<sup>2</sup>W. Helfrich and H. J. Deuling, *J. Phys. (Paris) Colloq.* **36**, C1-327 (1975).

<sup>3</sup>F. C. Frank, *Discuss. Faraday Soc.* **25**, 19 (1958).

<sup>4</sup>Ou-Yang Zhong-Can and Liu Jixing, *Phys. Rev. Lett.* **65**, 1679 (1990).

<sup>5</sup>N. Nakashima, S. Asakuma, J.-M. Kim, and T. Kunitake, *Chem. Lett.* **1984**, 1709 (1984).

<sup>6</sup>K. Yamada, H. Ihara, T. Ide, T. Fukumoto, and C. Hirayama, *Chem. Lett.* **1984**, 1713 (1984).

<sup>7</sup>N. Nakashima, S. Asakuma, and T. Kunitake, *J. Am. Chem. Soc.* **107**, 509 (1985).

<sup>8</sup>P. Yager and P. Schoen, *Mol. Cryst. Liq. Cryst.* **106**, 371 (1984).

<sup>9</sup>P. Yager, P. Schoen, C. Davies, R. Price, and A. Singh, *Biophys. J.* **48**, 899 (1985).

<sup>10</sup>J.-H. Fuhrhop, P. Schneider, E. J. Boekema, and W. Helfrich, *J. Am. Chem. Soc.* **110**, 2861 (1988).

<sup>11</sup>R. M. Servuss, *Chem. Phys. Lipids* **46**, 37 (1988).

<sup>12</sup>J. M. Schnur *et al.*, *Thin Solid Films* **152**, 181 (1987).

<sup>13</sup>J. M. Schnur *et al.*, (unpublished).

<sup>14</sup>W. Helfrich, *J. Chem. Phys.* **85**, 1085 (1986).

<sup>15</sup>P.-G. de Gennes, *C. R. Acad. Sci. Paris* **304**, 259 (1987).

<sup>16</sup>W. Helfrich and J. Prost, *Phys. Rev. A* **38**, 3065 (1988).

<sup>17</sup>A full theory in which we consider all the terms of Frank free energy for deriving the energy for TLB and TCLB has been obtained and will be published in the future.

<sup>18</sup>C. E. Weatherburn, *Differential Geometry of Three Dimensions* (Cambridge University Press, London, 1955), Vol. 1, p. 220.

<sup>19</sup>Ou-Yang Zhong-can and W. Helfrich, *Phys. Rev. A* **39**, 5280 (1989).

<sup>20</sup>A detailed derivation of Eqs. (15) and (80) may be seen, e.g., in a recent paper by Ou-Yang Zhong-can, Sen Liu, and Xie Yu-Zhang, [*Mol. Cryst. Liquid. Cryst.* (to be published)].

<sup>21</sup>P. G. de Gennes, *The Physics of Liquid Crystals* (Clarendon, Oxford, 1974).

<sup>22</sup>M. Spivak, *A Comprehensive Introduction to Differential Geometry* (Publish or Perish, Berkeley, 1979), Vol. 3, Chap 4.